IOP Conference Series: Earth and Environmental Science

PAPER • OPEN ACCESS

1D-3D co-simulation pipe resonance induced by cavitating vortex shedding

To cite this article: S Alligne *et al* 2024 *IOP Conf. Ser.: Earth Environ. Sci.* **1411** 012057

IOP Conf. Series: Earth and Environmental Science **1411** (2024) 012057 doi:10.1088/1755-1315/1411/1/012057

1D-3D co-simulation pipe resonance induced by cavitating vortex shedding

S ALLIGNE[1], N VEUTHEY[1], A BÉGUIN[1], N RUCHONNET[2], C NICOLET[1]

[1] Power Vision Engineering Sàrl, St-Sulpice, Switzerland
[2] ANDRITZ Hydro AG, Vevey, Switzerland
e-mail: sebastien.alligne@powervision-eng.ch

Abstract. Hydraulic systems may experience excitation caused by complex flow patterns within various components of the system. A computational effective way to predict the interaction between the hydraulic system and the excitation source is to conduct a co-simulation using two independent simulation codes. One code models the fluid pipe system using a one-dimensional compressible approach, while the other code simulates the excitation source with a three-dimensional model. Recognized as a standard communication protocol for linking two simulation codes that solve a system of ordinary differential equations, the Functional Mockup Interface, FMI, protocol has been implemented in SIMSEN to couple with the Ansys CFX software solution. Localized hydrodynamic instabilities including cavitation are prone to interact with the entire system. A cavitating case study has been investigated to assess robustness and accuracy of the co-simulation performed with the FMI protocol. The case study consists in a straight pipe connecting two constant pressure tanks with a bluff body placed at 3/4 of the pipe length. The vortex shedding is the excitation which frequency is proportional to the flow velocity. Measurements are available for resonant and non-resonant conditions in cavitating and free cavitating flow regimes. Co-simulations are performed between SIMSEN 1D model of the pipe and a pseudo 3D CFX model of the bluff body, reduced to one cell in the width direction. The comparisons with measurements show good agreement despite the pseudo 3D approach to simulate bluff body-induced excitation. This demonstrates that this approach is valid to address complex unsteady, compressible and cavitating flow phenomena.

1. Introduction

To characterize the dynamic behavior of the hydraulic system in a given power plant, a one-dimensional (1D) model of the system is used. However, 1D approch is not sufficient for modelling excitations caused by complex flow structures within a component of the system. Therefore, a three-dimensional (3D) numerical model is necessary. To capture the interaction between the hydraulic system and the excitation source, a co-simulation between two independent simulation codes must be performed. One code models the hydraulic system in 1D with a compressible flow approach, while the other simulates the 3D flow in the specific component of the hydraulic system that generates the excitation. In hydraulic machines, phenomena such as cavitation vortex ropes in the draft tube [1]-[8], rotating stalls or pressure fluctuations in the S-shaped region [9]-[12] are cases where 1D-3D coupling is particularly relevant. To simulate such strong coupling with hydraulic system, the FMI (Functional Mock-up Interface) co-simulation protocol has been implemented in SIMSEN software to be able to be coupled with ANSYS-CFX. This FMI coupling feature has been assessed for simulation of resonance phenomenon induced by a localized cavitating and unsteady flow structure in a hydraulic system.

2. Case study

To assess capability of FMI co-simulation, an experimental setup at the Laboratory for Hydraulic Machines at EPFL was used as a case study [13]. The experiment aimed to investigate hydroacoustic resonance in a pipe caused by flow perturbations. The hydroacoustic resonator consists of a square-cross-section PVC pipe connecting two tanks, as illustrated in Figure 1. The main geometrical parameters of the setup are provided in Table 1. A semi-circular bluff body, mounted perpendicular to the flow and located at three-quarters of the pipe length, generates the flow perturbation. Its rounded side faces upstream, while the flat side faces downstream. A variable-speed pump controls the flow velocity in the pipe, and the hydrostatic pressure is regulated using a vacuum pump connected to the downstream tank.

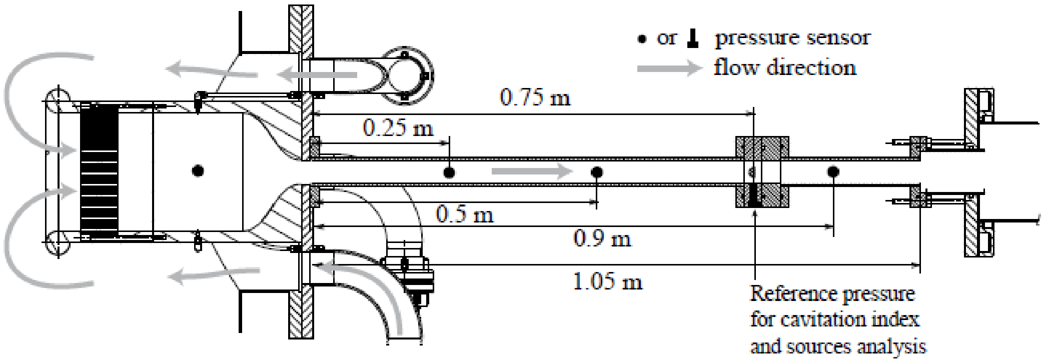

Figure 1. Experimental setup and pressure sensor position [13].

Table 1. Geometrical parameters of the experimental test case

Parameter	Symbol	Unit	Value
Pipe length	L	m	1.05
Pipe width	W	mm	40
Hydraulic diameter	D_h	mm	40
Wall thickness	e	mm	2
Position of bluff body	x_{bb}/L	-	0.75
Diameter of bluff body	D	mm	20
Cavitation free natural frequency	f_n	Hz	96.5
Measured cavitation incipience	σ_i	-	9
Reynolds number at pipe inlet	Re	-	60'000
Wave speed	a	m/s	202.65

3. Co-simulation between 1D and quasi-2D numerical models

3.1. Computational domain definition

The square pipe is divided in two sub-domains for the FMI co-simulation of the water hammer : the upstream part of the system is modelled in the 1D SIMSEN software whereas the downstream part including the excitation source induced by the bluff body's vortex shedding is modelled in Ansys CFX. The computational domain separation, schematised in Figure 2, is a compromise between accuracy, simplicity and computational cost by defining interface between the two domains upstream to the bluff body at four times the diameter D of the half-cylinder.

Figure 2. Computational domain separation for co-simulation.

3.2. *Quasi-2D numerical model*

The downstream part of the investigated system is modelled with a quasi-2D numerical model solving the Reynolds Averaged Navier Stokes equations for compressible flows that read:

$$\frac{\partial \bar{\rho}}{\partial t} + \frac{\partial(\bar{\rho}\widetilde{C_i})}{\partial x_i} = 0 \quad (1)$$

$$\frac{\partial(\bar{\rho}\widetilde{C_i})}{\partial t} + \frac{\partial}{\partial x_j}(\bar{\rho}\widetilde{C_i}\widetilde{C_j}) = -\frac{\partial \bar{p}}{\partial x_i} + \frac{\partial \overline{\sigma_{ij}}}{\partial x_j} + \frac{\partial \tau_{ij}}{\partial x_j} \quad (2)$$

Where ρ, C, p are density, velocity and static pressure of the liquid, $\overline{\sigma_{ij}}$the viscous stress tensor and $\tau_{ij}$the Reynolds stress term. The spatial domain is discretized with a mesh and differential equations are integrated over control volumes built around the mesh nodes. The used solver is ANSYS CFX. Two types of compressible liquid will be investigated in this paper depending on the simulated test case. The first one is the water single phase liquid which compressibility is defined by the barotropic law giving relation between pressure and density:

$$\frac{\partial \bar{\rho}}{\partial \bar{p}} = \frac{\bar{\rho}}{K} = \psi \quad (3)$$

$$\bar{\rho} = \rho_0 + \psi(\bar{p} - p_0) \quad (4)$$

Where $\rho_0$and p_0 are the reference density and pressure, K the bulk modulus. The bulk modulus is considered as constant and the wave speed propagation in the 3D numerical model is given by:

$$a = \sqrt{\frac{K}{\bar{\rho}}} \quad (5)$$

Hence only the elasticity of the fluid is taken into consideration and not pipe wall deformation. This fluid compressibility is combined with cavitation modelling since cavitation is expected to occur in the centre of the von Karman vortices for some operating points. The homogeneous ZGB cavitation model is used with no free surface model. The turbulence model used is SST while the turbulence numeric and the advection scheme are high resolution and the transient scheme is second backward Euler. The maximum number of coefficient loops is 10. The hydrodynamic domain is modelled in ANSYS CFX 2023R1. When cavitation is modelled, the heat transfer model is set as isothermal and not based on total energy, as it was found to help numerical stability. The computational domain is a quasi-2D domain defined by a 2D mesh swept with one cell of 1mm thickness in the width direction. A velocity profile is imposed as inlet boundary condition. To define this velocity profile, a preliminary steady simulation is performed with a quasi-2D long computational domain of the square pipe without bluff body. The outlet velocity profile of this preliminary computation is then used as inlet boundary condition for the co-simulation. To account for inlet flow rate variation imposed by the 1D numerical model during co-simulation, a linear scaling factor α is applied to the velocity profile. This factor is defined by the ratio between the flow rate coming from the 1D numerical model and the initial flow rate value corresponding to the investigated operating point. At the outlet, a static pressure outlet boundary condition with relative pressure is set, with the value of the relative pressure depending on the operating point investigated. The adequate outlet pressure is set to get the target pressure below the bluff body defined by the σ value according to the following equation :

$$\sigma = \frac{p_{bb} - p_v}{\frac{1}{2}\rho C^2} \rightarrow p_{bb} = \frac{1}{2}\rho C^2 + p_v \quad (6)$$

The incipient cavitation number σ_i found in the numerical investigations does not correspond to the experimental value. Therefore, a corrected cavitation number σ_{corr} is used for matching the targeted operating points. It is defined with respect to the measured and simulated incipient cavitation numbers σ_i^{meas} and σ_i^{sim}:

$$\sigma_{corr} = \frac{\sigma_i^{sim}}{\sigma_i^{meas}} \cdot \sigma = 1.78 \cdot \sigma \quad (7)$$

The correction factor is thus higher than the value of 1.28 found by Ruchonnet [13], which is most likely due to the fact that in the current study the hydrodynamic domain is modelled in quasi-2D approach and not in 3D. Before performing the co-simulation, the quasi-2D model is initialized by a standalone unsteady simulation which outlet pressure has been preliminary calibrated to get target σ value. Figure 3 shows the flow structure simulated by the quasi-2D domain.

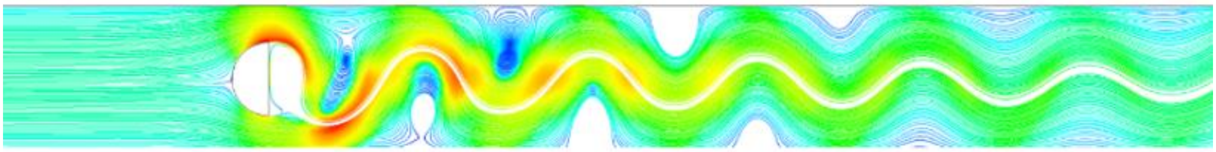

Figure 3. Simulation results of vortex shedding with the quasi-2D domain.

3.3. *1D numerical models*

To simulate hydraulic transients in hydraulic system, the momentum and the continuity equations are solved by neglecting the convective terms and assuming plane pressure wave and uniform velocity field in a cross section. This leads to the hyperbolic partial differential equations to be solved for the pipes, see Wylie and Streeter.

$$\frac{\partial h}{\partial t} + \frac{a^2}{gA} \cdot \frac{\partial Q}{\partial x} = 0 \quad (8)$$

$$\frac{\partial h}{\partial x} + \frac{1}{gA} \cdot \frac{\partial Q}{\partial t} + \frac{\lambda |Q|}{2gDA^2} \cdot Q = 0 \quad (9)$$

The variables h and Q represent the piezometric head and the discharge, respectively. In this study, these equations are solved using the SIMSEN simulation software developed by EPFL. The system of equations is solved using the Finite Difference Method, with a first-order centred scheme for spatial discretization and a Lax scheme for the discharge. This approach results in a system of ordinary differential equations that can be modelled as a T-shaped electrical equivalent circuit for the pipe element, as described by Nicolet [14]. The numerical models of the other hydraulic components are also based on an equivalent electrical scheme representation. The system of equations is set-up using Kirchoff laws and time domain integration of the full system is achieved by a Runge-Kutta 4th order procedure. The 1D numerical model, modelling the upstream part of the system, is composed of one pipe element between two reservoirs. This pipe element is spatially discretized by defining a number of pressure nodes Nb which is set to 40. Before performing the co-simulation, the 1D model is initialized by adjusting the upstream reservoir level to get target flow rate corresponding to the investigated operating point. The downstream reservoir level is defined by the total pressure computed at the inlet of the CFX domain which has been initialized to get target pressure below the bluff body corresponding to the investigated σ value.

3.4. *FMI coupling process*

The FMI (**F**unctional **M**ock-Up **I**nterface) is a co-simulation standard for coupling two simulation tools of dynamic systems. In SIMSEN, FMI co-simulation is available as a library, and offers both the 'master' and 'slave' mode. In this present study, SIMSEN was used as a co-simulation 'slave' and was linked to the ANSYS CFX 'master' tool using the FMI co-simulation standard. Figure 4 shows the exchanged data between the 1D and quasi-2D sub-domains during the co-simulation. The flow rate at the output of the 1D domain defines the input boundary condition of the quasi-2D domain, while the energy at the input of the quasi-2D domain defines the output boundary condition of the 1D domain.

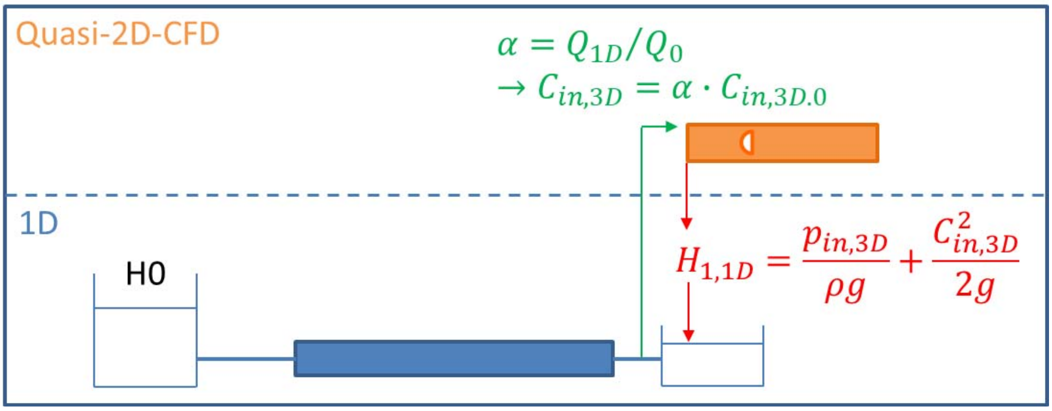

Figure 4. Exchanged data between 1D and quasi-2D domains during co-simulation.

The time step in the CFX quasi-2D domain is driven by the lift frequency f_L of the vortex shedding. For a Strouhal number St of 0.39, which is relatively high due to the confinement in the system, a lift frequency value of $f_L = St \cdot C/D = 58.5\, Hz$ is found for a reference velocity C set at 3 m/s. By considering ~40 time steps per period to get enough resolution for waterfall power spectral density analysis (PSD), this leads to a time step value of $\Delta t_{3D} = 4 \cdot 10^{-4}$ s. In the 1D domain, the time step is driven by the CFL criterion since the Runge-Kutta 4th order scheme is an explicit scheme. This leads to a time step value of $\Delta t_{1D} = 8.73 \cdot 10^{-5}$ s. It has been found that the time steps must be equal in both domains when dealing with Simsen-CFX FMI co-simulations, in order to prevent the occurrence of numerical instabilities. Therefore, the time discretisation in the hydrodynamic domain is decreased and set to $\Delta t_{3D} = \Delta t_{1D} = 8 \cdot 10^{-5}$ s.

4. Results

Four operating points, selected through the work of Ruchonnet [13], have been simulated, in cavitation-free and cavitating conditions, both in and out of resonance. The aim is to assess capability of SIMSEN-CFX FMI co-simulations to deal with resonance phenomenon in case of excitation of the 1D system by complex cavitating flow structure.

4.1. Cavitation free conditions

In cavitation-free condition, two operating points are investigated. The first one, defined by a flow velocity of 3m/s, is out of resonance condition where the shedding frequency f_s, being twice the lift frequency f_L , is higher than the natural frequency of the square pipe. To set the system in resonance condition with the first natural frequency of the pipe, the flow velocity is reduced to 2.54 m/s. The resulting flow parameters of these two operating points are given in Table 2.

Table 2. Flow condition parameters of cavitation-free operating points

Variable	Unit	Out of resonance	In resonance
C	m/s	3	2.54
f_s/f_n	-	1.18	0.99
St	-	0.38	0.38
σ_{corr}/σ_i	-	1.96	1.40

Figure 5 shows the Power Spectral Density (PSD) and the time series of the pressure coefficient fluctuations c_p' at the middle of the square pipe in out of resonance conditions. In this figure, results are compared to Ruchonnet's simulations [13] who performed both one way and coupled simulations. The one way simulation consists by performing a 3D CFD simulation from which, time series of predefined 1D parameters are extracted and injected afterwards in the 1D model to assess the system response. The two-way simulation is similar in terms of exchanged parameters but boundary conditions of 3D model

IOP Conf. Series: Earth and Environmental Science **1411** (2024) 012057 doi:10.1088/1755-1315/1411/1/012057

and 1D model are updated at each time step to account for interaction between the two domains. Hence, FMI co-simulation results should be compared with the two way simulation results from Ruchonnet. The same results are shown in resonance conditions in Figure 6. To visualize pressure fluctuations along the pipe length, the waterfall diagrams of c_p' PSD are plotted in Figure 7 for out of resonance and in resonance conditions. These waterfall diagrams can be compared to those obtained by Ruchonnet in Figure 8. It is shown that co-simulation is capable of reproducing the resonance conditions with the first natural mode of the square pipe in cavitation-free condition. Nevertheless, the amplitudes of the pressure fluctuations, whether in resonance conditions or not, are much greater than amplitudes predicted by Ruchonnet which are in agreement with the experimental measurements. In addition to higher amplitudes, a periodic response of the system is predicted which grows exponentially in case of resonance condition, see Figure 7.b. The quasi-2D model predicts periodic excitation source which is not the case for the Ruchonnet's 3D CFD model. Despite these differences in amplitude, location of maximum amplitude is found in the middle of the square pipe which is in agreement with measurements and Ruchonnet's results.

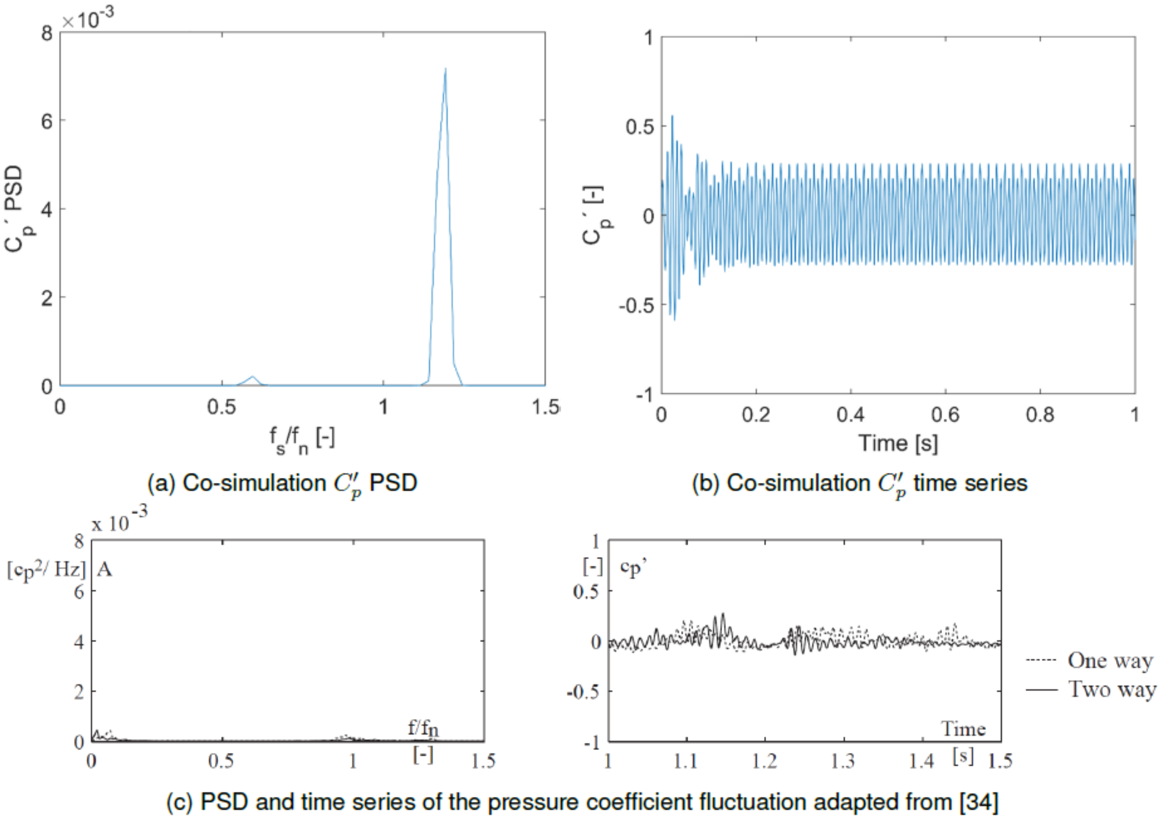

Figure 5. Power Spectral Density (PSD) analysis (a) and time series (b) of c_p' at $L/L_{tot} = 0.53$ in cavitation-free and out of resonance condition. Comparison with Ruchonnet's results [13] (c).

IOP Conf. Series: Earth and Environmental Science **1411** (2024) 012057 doi:10.1088/1755-1315/1411/1/012057

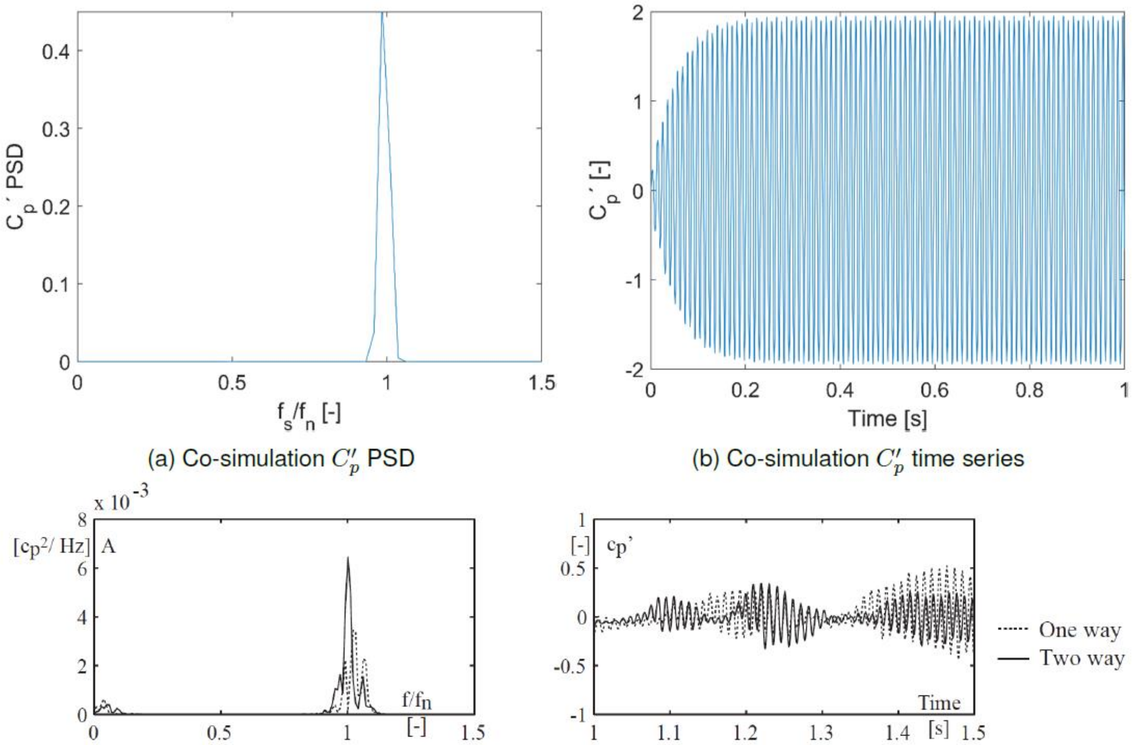

(a) Co-simulation C_p' PSD (b) Co-simulation C_p' time series

(c) C_p' PSD and time series adapted from [34]

Figure 6. Power Spectral Density (PSD) analysis (a) and time series (b) of c_p' at $L/L_{tot} = 0.53$ in cavitation-free and in resonance condition. Comparison with Ruchonnet's results [13] (c).

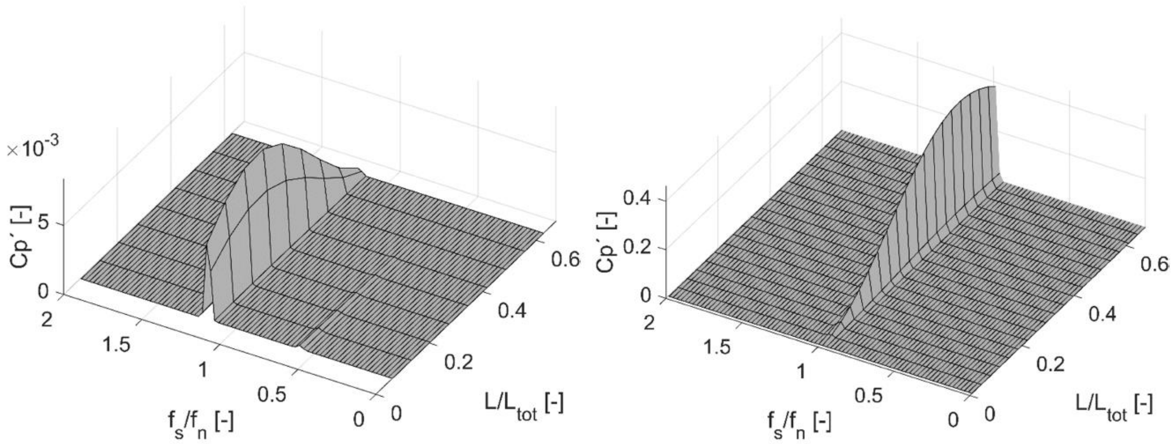

(a) Non-resonant (b) Resonant

Figure 7. Waterfall diagrams of c_p' Power Spectrum Density (PSD) in cavitation free condition for (a) out of resonance and (b) in resonance conditions.

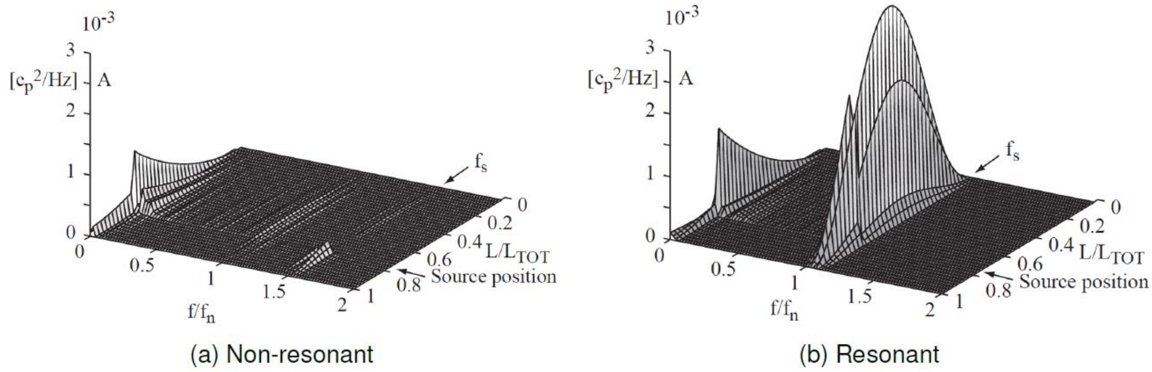

Figure 8. Ruchonnet's [13] waterfall diagrams of c_p' Power Spectrum Density (PSD) in cavitation free condition for (a) out of resonance (C=3.5m/s, fs/fn=1.52) and (b) in resonance conditions (C=2.5m/s, fs/fn=1.07).

4.2. Cavitating conditions

In this section, the resonance between the vortex shedding frequency and the square pipe will be investigated in presence of cavitation. Locally increasing the compressibility, cavitation reduces the natural frequencies of the system. Experiments show that the resonance occurs with the second eigenmode of the pipe, which in presence of cavitation has a value of $1.6 \cdot f_n = 154.4\,Hz$. Two operating points have been investigated from Ruchonnet's work [13]. The first one corresponds to the same operating point studied in the previous section with a flow velocity of 3m/s but with the presence of cavitation by reducing the Thomas number. This point is found experimentally to be out of resonance whereas the second operating point is in resonance condition with the flow velocity increased to 3.27 m/s to set the resonance with the second eigenmode of the square pipe. The resulting flow parameters of these two operating points are given in Table 3. Co-simulations of these two operating points have been performed and contrary to experiments, the response to the source excitation is amplified for the flow velocity of 3m/s which is supposed to be out of resonance. Compared to the cavitation-free condition with the same flow velocity, the presence of cavitation has slightly increased the Strouhal number from 0.38 to 0.43 leading to a system response amplification at a frequency value of $1.35 \cdot f_n = 130.3\,Hz$.

Table 3. Flow condition parameters of cavitation operating points

Experimentally expected		Out of resonance	In resonance
Found numerically as		Near resonance	Out of resonance
Variable	Unit		
C	m/s	3	3.27
f_s/f_n	-	1.34	1.59
St	-	0.43	0.47
σ_{corr}/σ_i	-	0.84	0.78

To visualize pressure fluctuations along the pipe length, the waterfall diagrams of c_p' PSD are plotted in Figure 9 a) and b) for the two operating points. For reasons of numerical stability issues, the two-way simulation could not be carried out by Ruchonnet due to the explicit scheme nature of the coupling algorithm. Hence one-way simulation results, presented in Figure 9 c), are used for comparison. Contrary to simulations in cavitation-free condition, the order of magnitudes of the system response are similar to the Ruchonnet's one-way simulation results. Under these cavitation conditions, the natural frequency of the system is predicted with a deviation of 16% from Ruchonnet's experimental results. In addition, the location of the maximum amplitude is predicted at 0.4 times the length of the pipe, whereas the experiment shows a maximum at the first third of the pipe. These differences in terms of frequency and position of the pressure maximum suggest that resonance has not necessarily been reached, but that the conditions are close. Additional calculations at other σ values would make it possible to identify the exact resonance. Co-simulation seems to be capable of simulating resonance phenomenon involving cavitating unsteady flows.

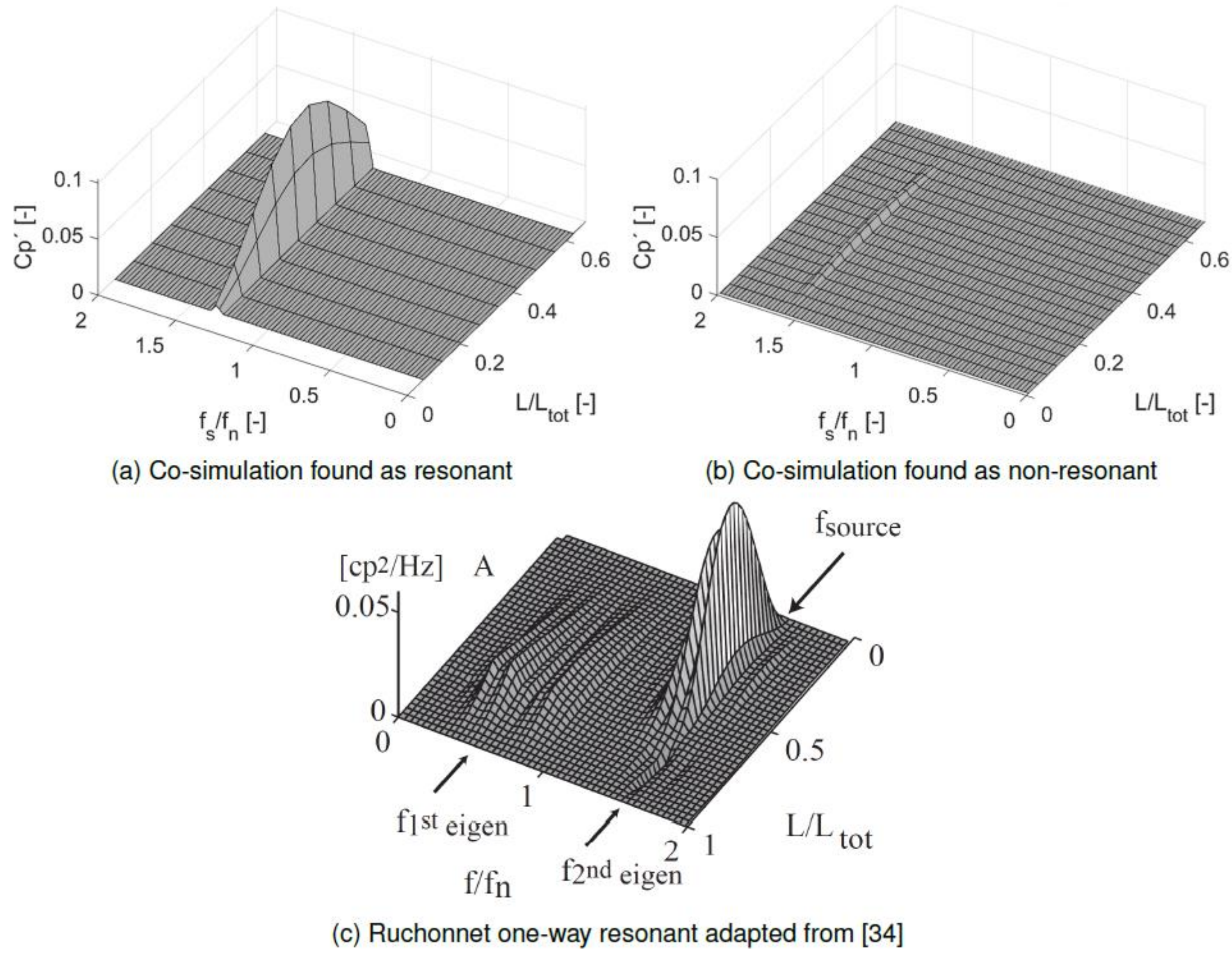

Figure 9. Waterfall diagrams of c_p' Power Spectrum Density (PSD) in cavitation condition for (a) expected out of resonance condition but found as resonant and (b) in expected resonance condition but found as out of resonance.

5. Conclusion

Co-simulation is of growing interest in the field of hydropower, in order to predict the interactions between the excitation induced by unsteady flows in the machines and the hydraulic system. The FMI communication protocol was therefore implemented in the SIMSEN software. It is now considered as a standard for communication between two independent codes. This functionality is also available in the commercial Ansys CFX solution, enabling the two software packages to be coupled for detailed transient studies. A case study, which consists in a straight pipe connecting two constant pressure tanks with a bluff body placed at 3/4 of the pipe length, has been used to assess the robustness of the FMI protocol in case of resonance phenomenon where strong interaction occurs between the 1D system model and the quasi-2D model of the excitation source. It is shown that resonance or near-resonance conditions can be simulated with or without cavitation in the flow structure of the excitation source. With cavitation in the quasi-2D domain, the system's eigenmodes are modified by decreasing natural frequencies. However, resonance under cavitation conditions have not been achieved despite the system having an amplified response to its excitation. This would require further calculations at additional σ values although FMI co-simulation is computational time-consuming due to small time step required.

6. References

[1] Ruprecht, Albert, Helmrich, Thomas, Aschenbrenner, Thomas, *et al.* Simulation of vortex rope in a turbine draft tube. In : *Proceedings of the 21st IAHR Symposium on Hydraulic Machinery and Systems*. EPFL/STI/LMH, Lausanne, Switzerland, 2002. p. 259-266.

[2] Cherny, Sergey, Chirkov, Denis, Bannikov, Denis, *et al.* 3D numerical simulation of transient processes in hydraulic turbines. In : *IOP Conference Series: Earth and Environmental Science*. IOP Publishing, 2010. p. 012071.

[3] Ruchonnet, Nicolas. *Multiscale computational methodology applied to hydroacoustic resonance in cavitating pipe flow*. EPFL, 2010.

[4] Alligné, Sébastien. *Forced and self-oscillations of hydraulic systems induced by cavitation vortex rope of Francis turbines*. EPFL, 2011.

[5] Chirkov, D., Avdyushenko, A., Panov, L., *et al.* CFD simulation of pressure and discharge surge in Francis turbine at off-design conditions. In : *IOP conference series: earth and environmental science*. IOP Publishing, 2012. p. 032038.

[6] Mössinger, P., Conrad, P., et Jung, A. Transient two-phase CFD simulation of overload pressure pulsation in a prototype sized Francis turbine considering the waterway dynamics. In : *IOP Conference Series: Earth and Environmental Science*. IOP Publishing, 2014. p. 032033.

[7] Chirkov, D., Panov, L., Cherny, S., *et al.* Numerical simulation of full load surge in Francis turbines based on three-dimensional cavitating flow model. In : *IOP Conference Series: Earth and Environmental Science*. IOP Publishing, 2014. p. 032036.

[8] Zhang, Xiaoxi, Chen, Qiuhua, et Liao, Jie. Dynamic evolutions between the draft tube pressure pulsations and vortex ropes of a Francis turbine during runaway. *International Journal of Fluid Machinery and Systems*, 2017, vol. 10, no 4, p. 404-411.

[9] Zhang, Xiao-xi et Cheng, Yong-guang. Simulation of hydraulic transients in hydropower systems using the 1-D-3-D coupling approach. *Journal of Hydrodynamics, Ser. B*, 2012, vol. 24, no 4, p. 595-604.

[10] Zhang, Xiao-xi, Cheng, Yong-guang, Yang, Jian-dong, *et al.* Simulation of the load rejection transient process of a francis turbine by using a 1-D-3-D coupling approach. *Journal of Hydrodynamics*, 2014, vol. 26, no 5, p. 715-724.

[11] Zhang, X. X., Cheng, Y. G., Xia, L. S., *et al.* Dynamic characteristics of a pump-turbine during hydraulic transients of a model pumped-storage system: 3D CFD simulation. In : *IOP Conference Series: Earth and Environmental Science*. IOP Publishing, 2014. p. 032030.

[12] Zhang, Xiaoxi, Cheng, Yongguang, Xia, Linsheng, *et al.* CFD simulation of reverse water-hammer induced by collapse of draft-tube cavity in a model pump-turbine during runaway process. In : *IOP Conference Series: Earth and Environmental Science*. IOP Publishing, 2016. p. 052017.

[13] Ruchonnet, *Multiscale Computational Methodology Applied to Hydroacoustic Resonance in Cavitating Pipe Flow*. EPFL, Lausanne, 2010. doi:10.5075/epfl-thesis-4778.

[14] Nicolet, Christophe. *Hydroacoustic modelling and numerical simulation of unsteady operation of hydroelectric systems*. EPFL, Lausanne, 2007.